IJAREEIE

e-ISSN: 2278-8875
p-ISSN: 2320-3765

International Journal of Advanced Research in Electrical, Electronics and Instrumentation Engineering

Volume 13, Issue 9, September 2024

INTERNATIONAL STANDARD SERIAL NUMBER INDIA

Impact Factor: 8.514

International Journal of Advanced Research in Electrical, Electronics and Instrumentation Engineering (IJAREEIE)

| e-ISSN: 2278 – 8875, p-ISSN: 2320 – 3765| www.ijareeie.com | Impact Factor: 8.514 | A Monthly Peer Reviewed & Refereed Journal |

|| Volume 13, Issue 9, September 2024 ||

| DOI:10.15662/IJAREEIE.2024.1309009 |

Contact Resistance and Cut-Off Frequency Estimation of the Organic Thin Film Transistors using Particle Swarm Optimization

Subodh Kumar, Rajeev Kumar Thakur

Department of Electronics and Communication, NRI Institute of Information Science and Technology, Bhopal, India

ABSTRACT: Organic thin-film transistors (OTFTs) are inexpensive, incredibly flexible devices utilized in printing, sensing, and displaying applications. Despite these benefits, OTFTs have some drawbacks, such as low cutoff frequency or speed, high contact resistance, To address these issues, an objective function that is taught by particle swarm optimization (PSO) has been created. By scaling the contact length, the overall performance will be evaluated at different channel lengths (length of drain and source electrode). Furthermore, scaling the contact length reveals that, in contrast to other approaches, PSO has enabled the lowest value of contact resistance and highest cut-off frequency. Furthermore, for larger contact length scaling in the roughly 80 nm region, a decrease in contact resistance and an increase in cut-off frequency continue.

KEYWORDS: OTFT, contact resistance, cutoff frequency, PSO, contact length

I. INTRODUCTION

ORGANIC thin film transistor is the greatest alternative to the traditional MOSFET transistor because of its flexible design, attractive electronics characteristics, and fast operation. Organic thin-film transistors with charge carriers often require thin films with strongly oriented features in order to perform well.

This study[1] takes into account the overlap of source-drain contacts on the organic semiconductor surface and the actual channels across the contacts to present mathematical models for top and bottom contacts . The suggested models look into the contact effect, and a two-dimensional numerical circuit modeling is used to confirm it. Results from analyses are contrasted with simulation and results from experiments, demonstrating high agreement and validating the models. The electrical properties are derived from the linear to saturated domain.

The paper [2] looked into the stagger organic thin-film transistors (OTFTs) interaction length scaling capabilities (with a length for both the source and drain electrode). We looked into how the Schottky barrier affected the source & drain. Report On the channel width, thickness of the semiconductors layer, access, asymmetry of mobility, chemical chaos, and gate-source voltage on contact duration scaling downward in addition to the electrode. We found that until the contact's length is below 500 nm, the contact resistance doesn't increase.

We compare the efficiency of single-gate and planar dual-gate conducting nanotube thin-film transistors (SNTFTs) in the article [3]. A thin layer of semiconducting carbon nanotubes with single walls with a 95% enrichment is applied to the outermost layer of hafnium oxide (HfO x) modified by amino-silane. The dielectric used for the SNTFT's rear gates is HfO x, which is deposited via radiofrequency sputtering, whereas SiO 2 is utilized for the top gates. Every SNTFT has demonstrated a linear zone operation and a p-type outputs distinctive behaviour with clear saturating.

The current work[4] investigates the static and dynamic behaviors of dual-gate organic transistors with thin films (DG-OTFTs) driven universal logic gates using an Atlas 2-D numerical circuit simulator. The electrical characteristics as well as the parameters of pentacene-based DG-OTFT are evaluated and validated with respect to previous experimental data.
.
In [5], a succinct description for the dc current and capacitor of organic thin-film transistors is given. It is based on the variable-range hopping-transport idea and is based on the double-exponential density-of-state functional. The suggested model may accurately capture the current shift away from the below-the-threshold domain to the linear and saturated domain with a single, coherent description. There is a good match between the pentacene field-effect transistor observations and theoretical computation. Additionally highlighted is the use of this little model for simulation of circuits[5].

| e-ISSN: 2278 – 8875, p-ISSN: 2320 – 3765| www.ijareeie.com | Impact Factor: 8.514 | A Monthly Peer Reviewed & Refereed Journal |

|| Volume 13, Issue 9, September 2024 ||

| DOI:10.15662/IJAREEIE.2024.1309009 |

In this paper[6], we employ a formula that we earlier derived to analyze the dependency of charge carrier mobility on heat in polymer TFTs, or PTFTs. This formula has a benefit over earlier expressions in that the majority of the model elements reflect physical device properties.

An enhanced small analytical current-voltage simulation of organic field-effect transistors (OFETs) is proposed in a research publication [7]. The proposed model can be included into circuit simulation programs of the SPICE type. We introduced a new hyperbolic formula that not only allows more accurate low-voltage current and conductance fitting, but also enhanced the output saturate behaviour. It was proposed to use a new term for the below the threshold current to account for all OFET operating regimes. A methodical strategy was used to extract all of the model's variables, and the reliability of the model across a broad operating range was confirmed by comparing the modelled current with data from experiments on pentacene-based OFETs.

According to the paper[8], charging in the devices under investigation takes place through state hopping. The outcomes obtained clearly show how the organic active layer deposition circumstances might enhance device efficiency. Ultimately, a mathematical framework has been created to comprehend the transport of charges in DBP-TFTs and to replicate how heat affects total resistance & current-voltage properties.

A novel DC/dynamic analytical approach to organic thin-film transistors (OTFTs) is introduced in this study [9]. The parameter range hopping principle, which describes thermally triggered carrier tunnelling between localised states, is the foundation of the concept. With just one formulation, it correctly takes into consideration operating situations that are below threshold, linear, and saturated. Additionally, the model is appropriate for CAD programs and doesn't need the explicit definition of the somewhat vaguely stated threshold and saturate voltages as the input parameters.

Because translucent organic thin-film transistors (OTFTs) enable concurrent optical images, electric detecting, and modification, they hold great promise for biological electronics applications. Modern transparent OTFTs, however, have limitations in their device efficiency because to their high threshold voltage and restricted mobility. The primary cause of this is the significant contact resistance brought about by an energy level imbalance that exists between organic semiconductors and clear electrodes. Here, we present transparent OTFTs that have had the electrode material of indium tin oxide changed by fluorinated silanes to enhance device functionality[10].

Robotics, control of processes, and workplace security are just a few of the many uses for large-area, flexible proximity-sensing panels. However, the existing systems are limited in their uses by the heavy and inflexible circuitry they normally require. In this project, we show a large-area, foldable proximity-sensing display with integrated analog front-end circuits in each pixels, composed of printable organic substances. The detecting surface of printed thin-film sensors are constructed from printable organic thin-film transistors as well as poly(vinylidene fluoride-co-trifluoroethylene) co-polymers[11].

Flexible electronic devices have shown to have a great deal of promise for improving convenience and enjoyment in everyday life. The development of flexible organic field-effect transistor (FOFET) technology for flexible detectors, rollable screens, bending smart cards, and synthetic skins has been the focus of intense attention. Unfortunately, due to a lack of established production techniques and common outstanding performance material stacks, numerous uses are still in their infancy. This paper provides a detailed summary of the material selection, device layout, and proven applications for FOFET devices and circuitry[12].

| e-ISSN: 2278 – 8875, p-ISSN: 2320 – 3765| www.ijareeie.com | Impact Factor: 8.514 | A Monthly Peer Reviewed & Refereed Journal |

|| Volume 13, Issue 9, September 2024 ||

| DOI:10.15662/IJAREEIE.2024.1309009 |

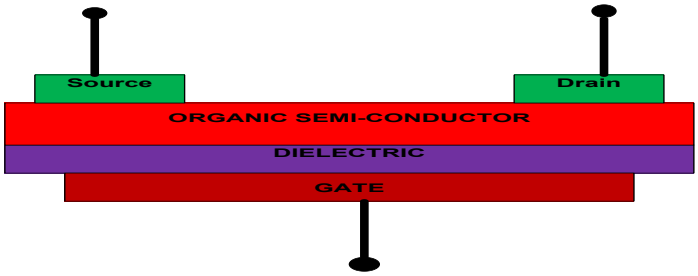

Fig.1 Structure of the OTFT

After finishing the thorough literature survey research, there were significant issues with OTFT. Overall study of the literature gaps indicates performance parameters such as large and incorrect contact resistance and low switching frequency under varying contact length. The suggested topic is unusual in that it uses particle swarm optimization (PSO) to optimize the performance parameters indicated above. The aforementioned performance criteria have been used to build an objective function, which PSO will further train. By adjusting the contact length to achieve the minimal value of contact resistance, the hybrid intelligent controller has enabled the PSO controller to achieve the maximum cut-off frequency when compared to previous techniques.

II. GENERAL STRUCTURE OF OTFT:

The gate position and organic contact determine potential OTFT geometries. The terms Top Gate and Top contact, Top Gate and bottom contact, Bottom Gate and Top contact, and Bottom Gate and bottom contact refer to the four different forms of feasible OTFT constructions.

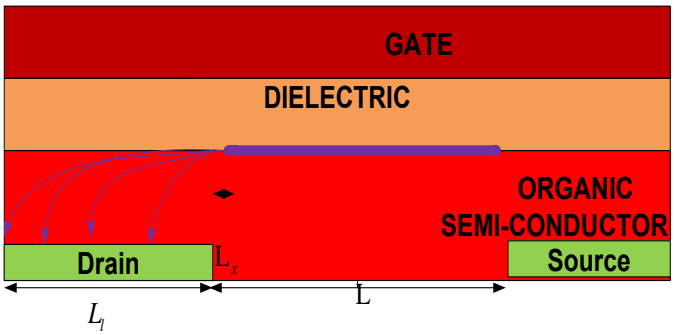

Fig.2 Top gate and bottom contact OTFT Structure

Fig. 2, which is exclusive to this work, shows the OTFT construction from a top view with the gate at its highest point.

The gate is placed above an insulator or dielectric, and a dielectric lies between the gate with the organic semiconductor. The source and drain of the OTFT are at the bottom. At the electrode's the edge, the channel current (Ids) begins spreading close to the drain connection.

The organic semiconductor sits in between the hydrophobic and the gate, and the barrier, or a dielectric, is placed above the gate. The source and drain of the organic semiconductors are at the bottom. The drain connection on the edge of the electrodes will be the destination of the channel's growing current.

There are certain common parameters like L is the length of the channel, L_x is the is the distance between spreading point and drain contact, L_l is the contact length (length of drain and source electrode).

| e-ISSN: 2278 – 8875, p-ISSN: 2320 – 3765| www.ijareeie.com | Impact Factor: 8.514 | A Monthly Peer Reviewed & Refereed Journal |

|| Volume 13, Issue 9, September 2024 ||

| DOI:10.15662/IJAREEIE.2024.1309009 |

III. PERFORMANCE PARAMETERS OF OTFT

The performance of the OTFT have been realized in terms of various performance parameters like contact resistance and cutoff frequency

3.1 Contact resistance(R_c)

To understand how contact length scaling influences the cut off frequency of OTFTs, it is crucial to look at the effect on contact resistance[2]. Assuming that the voltage at the point where the channel current begins to spread is the gate voltage and that the contact resistance close to the source/drain is normally in Eq.1, the source/drain contact resistance can be expressed as following.

$$R_c = \frac{V}{i_{ds}} \tag{1}$$

i_{ds} is the drain to source current which is shown in Eq.2

$$i_{ds} = \mu C_{ox} \frac{W}{L-2L_x}(V_{ds}-2V)(V_{gs}-\frac{(V_{ds}-2V)}{2}) \tag{2}$$

3.2 Cutoff frequency (f_T)

The cutoff frequency (f_T) will be expressed as mentioned in Eq.3 which increases with the decreases in the contact resistance [2].

$$f_T = \frac{\mu_{effec}(V_{gs}-V_{th})}{2\pi L(L+2L_l)} \tag{3}$$

IV. DESIGN OF PARTICLE SWARM OPTIMIZATION

An evolutionary optimization strategy is the PSO approach. Because of its exceptional computational power, it is a well-liked option for numerous technical uses. The PSO method converges more quickly and consistently than other approaches that utilize populations stochastic optimization, making it a quick means to ascertain the makeup of the system.

The PSO algorithm consists of the following three primary steps:

i) Figuring out how fit each particle is.

ii) Changing each particle's position and speed in order to improve local and global ideal fitness and positioning.

iii) For the purpose of optimizing the PSO algorithm, the flowchart gives updates on the particle's position and velocity.

The general expression for the location and velocity particles in the subsequent iteration is given by equations 4 and 5.

$$v(t+1) = \omega(t)v(t) + c_1 r_1(pbest(t) - x(t)) + c_2 r_2(gbest(t) - x(t)) \tag{4}$$

$$x(t+1) = x(t) + v(t+1) \tag{5}$$

where t is the current value of the iteration. ω, the inertial weight parameter, is a function of t. There are two uniforms, r1 and r2, and for each, there is a random number between 0 and 1. C1 and C2 are the two accelerometer coefficients.

| e-ISSN: 2278 – 8875, p-ISSN: 2320 – 3765| www.ijareeie.com | Impact Factor: 8.514 | A Monthly Peer Reviewed & Refereed Journal |

|| Volume 13, Issue 9, September 2024 ||

| DOI:10.15662/IJAREEIE.2024.1309009 |

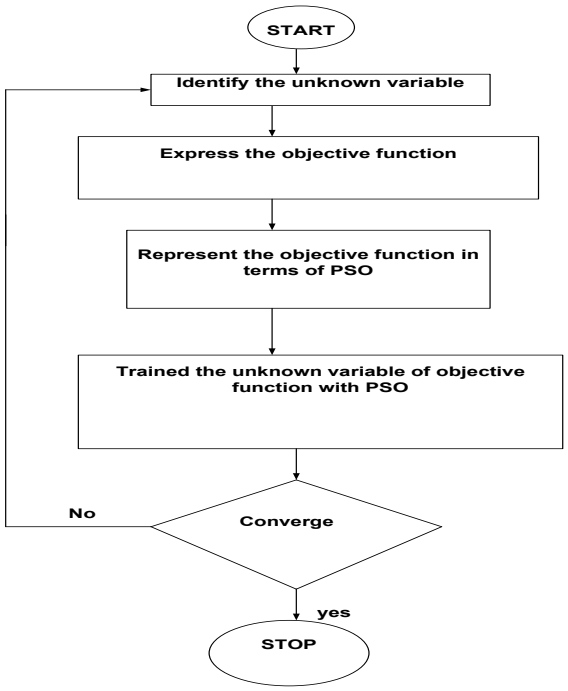

Fig.3 Various steps of PSO for the controlling of induction motor.

V. IMPLEMENTATION OF PARTICLE SWARM OPTIMIZATION

The formulation of objective functions begins by considering the Eq.1, 2 and Eq.3. and objective function is mathematically expressed as shown in Eq.6

$$f(k_1,k_2,k_3,k_4)=k_1 e^{-(R_c+k_2\frac{V}{i_{ds}})}+k_3 e^{-(f_T+k_4(V_{gs}-V_{th}))} \quad (6)$$

Eq.6 can be modified which is expressed in Eq.7 by expanding the exponential function

$$f(k_1,k_2,k_3,k_4)=k_1(1-R_c)+k_1k_2\frac{V}{i_{ds}}+ +k_3(1-f_T)+k_3k_4(V_{gs}-V_{th}) \quad (7)$$

Compare the Eq..7 with Eq.4, it is obtained as shown below from Eq.8 to Eq.11

$$v(t+1)=f(k_1,k_2,k_3,k_4) \quad (8)$$

$$c_1r_1(pbest(t)-x(t))=k_1(1-R_c) \quad (9)$$

$$c_2r_2(gbest(t)-x(t))=k_3(1-f_T) \quad (10)$$

$$\omega(t)v(t)=k_1k_2\frac{V}{i_{ds}}+k_3k_4(V_{gs}-V_{th}) \quad (11)$$

The unknown parameters k_1,k_2,k_3,k_4 will be trained by using PSO

| e-ISSN: 2278 – 8875, p-ISSN: 2320 – 3765| www.ijareeie.com | Impact Factor: 8.514 | A Monthly Peer Reviewed & Refereed Journal |

|| Volume 13, Issue 9, September 2024 ||

| DOI:10.15662/IJAREEIE.2024.1309009 |

VI. PERFORMANCE PARAMETRIC EVALUATION OF THE OTFT

The design and implementation of PSO has been discussed in the previous section. The change in channel length also affects the change in contact length or vice-versa. There are lot of characteristics plotted which shows the effects of change in channel length and contact length. The variation of contact resistance with contact length(nm) under the channel length of (L=9µm, 4µm,) with PSO which is shown in Fig.4 and Fig.5

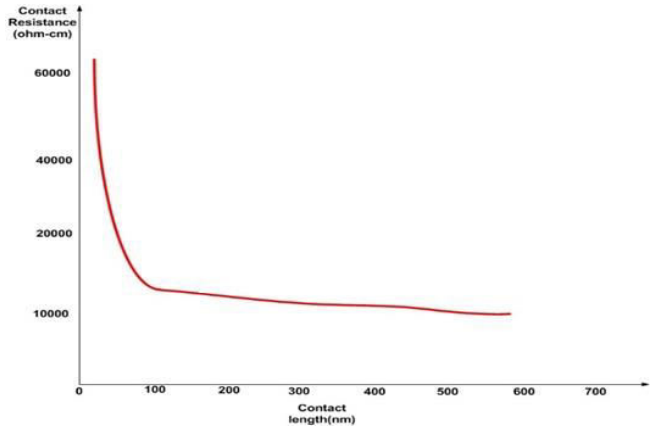

Fig.4 Variation of contact resistance with contact length by using PSO at channel length (L=9µm)

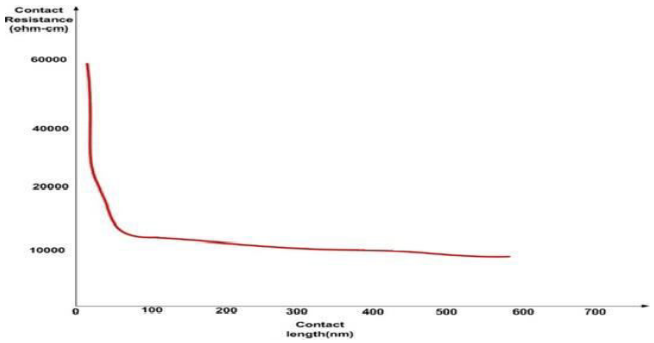

Fig.5 Variation of contact resistance with contact length by using PSO at channel length (L=4µm)

Similarly, the variation of cut off frequency (Hz) with contact length(nm) under the channel lengths of (L=9 µm, 4µm, and 2µm) with PSO have been reflected from Fig.6 and Fig.7. It is observed that cut off frequency is gradually increasing approximately up to 80nm with the increase in the contact length(nm), thereafter decreases.

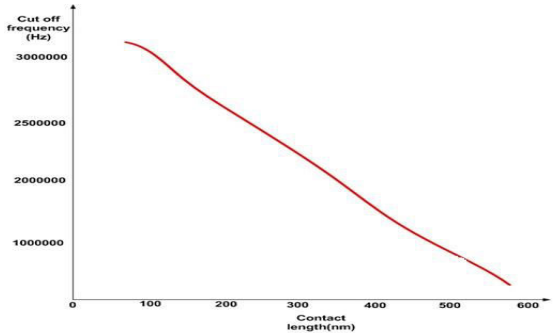

Fig.6 Variation of cutoff frequency with contact length by using PSO at channel length (L=9µm)

| e-ISSN: 2278 – 8875, p-ISSN: 2320 – 3765| www.ijareeie.com | Impact Factor: 8.514 | A Monthly Peer Reviewed & Refereed Journal |

|| Volume 13, Issue 9, September 2024 ||

| DOI:10.15662/IJAREEIE.2024.1309009 |

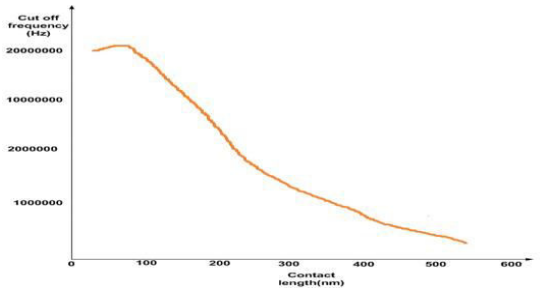

Fig.7 Variation of cutoff frequency with contact length by using PSO at channel length (L=4µm)

The different values of contact resistance corresponding to the different value of the contact length for L=9 um under different methods is shown in Table.1 and its graphical comparison is shown in Fig.8

Table.1 Contact resistance values at different contact lengths with PSO at channel length (L=9µm)

Contact length(nm)	PSO	Method [2]
55	19000	22100
70	10000	20100
90	14500	16100
140	13100	15100

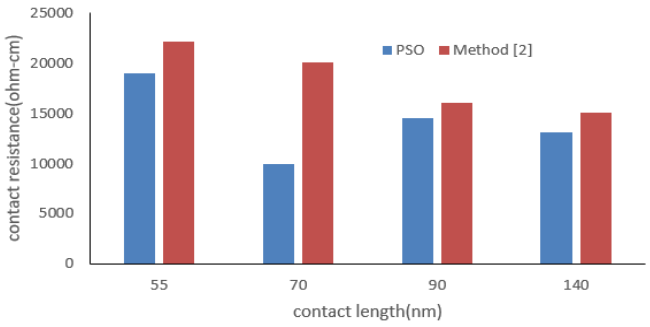

Fig.8 Comparison of variation of contact resistance with contact length with PSO at channel length (L=9µm)

The different values of contact resistance corresponding to the different values of the contact length for L=4 um using PSO is shown in Table.2 and its graphical comparison is shown in Fig.9

Table.2 Contact resistance values at different contact lengths with PSO at channel length (L=4µm)

Contact length (nm)	PSO	Method [2]
55	17500	21600
70	12800	16900
90	11500	15600
140	10600	14700

| e-ISSN: 2278 – 8875, p-ISSN: 2320 – 3765| www.ijareeie.com | Impact Factor: 8.514 | A Monthly Peer Reviewed & Refereed Journal |

|| Volume 13, Issue 9, September 2024 ||

| DOI:10.15662/IJAREEIE.2024.1309009 |

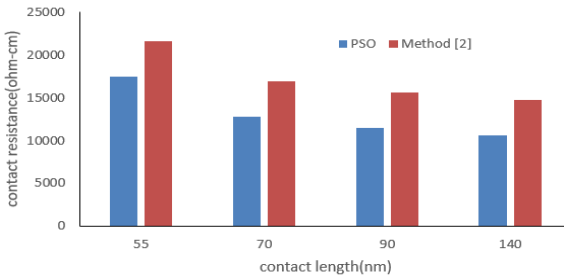

Fig.9 Comparison of variation of contact resistance with contact length with PSO at channel length (L=4µm)

Similarly,The different values of contact resistance corresponding to the different value of the contact length for L=9 um under different methods is shown in Table.3 and its graphical comparison is shown in Fig.10. The different values of contact resistance corresponding to the different values of the contact length for L=4 um using PSO is shown in Table.4 and its graphical comparison is shown in Fig.11

Table.3 Cutoff frequencies variation at different contact lengths with PSO at channel length (L=9µm)

Contact length (nm)	PSO	Method [2]
55	3000000	2700000
70	3600000	3002100
90	2800000	2202100

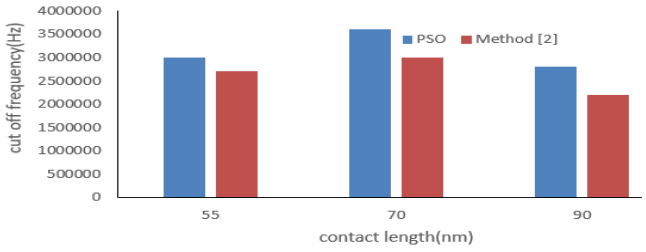

Fig.10 Comparison of variation of cut off frequency with contact length with PSO at channel length (L=9µm)

Table.4 Cutoff frequencies variation at different contact lengths with different methods at channel length (L=4µm)

Contact length (nm)	PSO	Method [2]
55	1800000	1400000
70	2800000	2100000
90	3300000	3150000

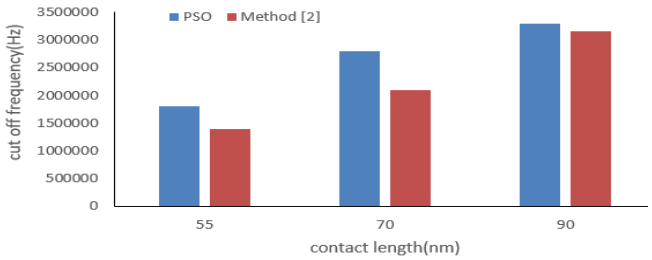

Fig.11 Comparison of variation of cut off frequency with contact length with PSO at channel length (L=4µm)

| e-ISSN: 2278 – 8875, p-ISSN: 2320 – 3765| www.ijareeie.com | Impact Factor: 8.514 | A Monthly Peer Reviewed & Refereed Journal |

|| Volume 13, Issue 9, September 2024 ||

| DOI:10.15662/IJAREEIE.2024.1309009 |

VII. CONCLUSION

OTFTs, or organic thin-film transistors, are very flexible, low-cost semiconductors used in printing, sensing, and display applications. OTFTs have certain disadvantages despite these advantages, including low cutoff frequency or speed, high contact resistance, An objective function trained by particle swarm optimization (PSO) has been developed to tackle these problems. The overall performance will be assessed at various channel lengths (length of source and drain electrode) by scaling the contact length. Moreover, scaling the contact length shows that PSO has enabled the highest cut-off frequency and lowest contact resistance value compared to other methods. Moreover, a drop in contact resistance and an increase in cut-off frequency persist for longer contact length scaling in the about 80 nm range.

REFERENCES

[1] B. Kumar, B. K. Kaushik, and Y. S. Negi, "Modeling of top and bottom contact structure organic field effect transistors", Journal of Vacuum Science and Technology B: Microelectronics and Nanometer Structures, Vol. 31, No. 1, pp. 012401-1–012401-7, Jan. 2013.
[2] Hong Wang, Wei Wang, Pengxiao Sun, Xiaohua Ma, Ling Li, Ming Liu, and Yue Hao, "Contact Length Scaling in Staggered Organic Thin-Film Transistors," IEEE Electron Device Letters, vol. 36, no. 6, pp. 609-611, 2015.
[3] K. C. Narasimha murthy and R. Paily, "Performance comparison of
single and dual gate carbon nanotube thin film field effect transistor",
IEEE Trans. on Elect. Development, Vol. 58, pp. 315323, 2011.
[4] B. Kumar, B. K. Kaushik and Y. S. Negi, "Static and dynamic characteristics of dual gate organic TFT based NAND and NOR circuits", Journal of Computational Electronics, Vol. 13, No. 3, pp.112, Sept. 2014
[5] L. Li, H. Marien, J. Genoe, M. Steyaert, and P. Heremans, "Compact
model for organic thin-film transistor," *IEEE Electron Device Lett.* vol. 31, no. 3, pp. 210–212, Mar. 2010.
[6] M. Estrada *et al.*, "Modeling the behavior of charge carrier mobility with
temperature in thin-film polymeric transistors," *Microelectron. Eng.*, vol. 87, no. 12, pp. 2565–2570, Dec. 2010.
[7] C. H. Kim *et al.*, "A compact model for organic field-effect transistors with improved output asymptotic behaviors," *IEEE Trans. Electron Devices*, vol. 60, no. 3, pp. 1136–1141, Mar. 2013.
[8] W. Boukhili, M. Mahdouani, R. Bourguiga, and J. Puigdollers, "Temperature dependence of the electrical properties of organic thin-film transistors based on tetraphenyldibenzoperiflanthene deposited at different
substrate temperatures: Experiment and modeling," *Microelectron. Eng.*,
vol. 150, no. 25, pp. 47–56, Jan. 2016.
[9] E. Calvetti, L. Colalongo, and Z. M. Kovács-Vajna, "Organic thin film transistors: A DC/dynamic analytical model," *Solid-State Electron.*,vol. 49, no. 4, pp. 567–577, 2005
[10] Yilun Zhong,Jiwei Zou,Taoming Guo,Lei Han,Ye Zou,Wei Tang, Yongpan Liu,Huazhong Yang,Yunlong Guo, Chen Jiang, Modification of Indium Tin Oxide Electrodes by Fluorinated Silanes for Transparent Organic Thin-Film Transistors, IEEE Electron Device Letters, vol.45, no.3,pp. 396 – 399, 2024
[11] M. Fattori, S. Cardarelli, J. Fijn, P. Harpe, M. Charbonneau, D. Locatelli, et al., "A printed proximity-sensing surface based on organic pyroelectric sensors and organic thin-film transistor electronics", Nature Electron., vol. 5, no. 5, pp. 289-299, May 2022.
[12] K. Liu, B. Ouyang, X. Guo, Y. Guo and Y. Liu, "Advances in flexible organic field-effect transistors and their applications for flexible electronics", *NPJ Flexible Electron.*, vol. 6, no. 1, pp. 1, Jan. 2022.

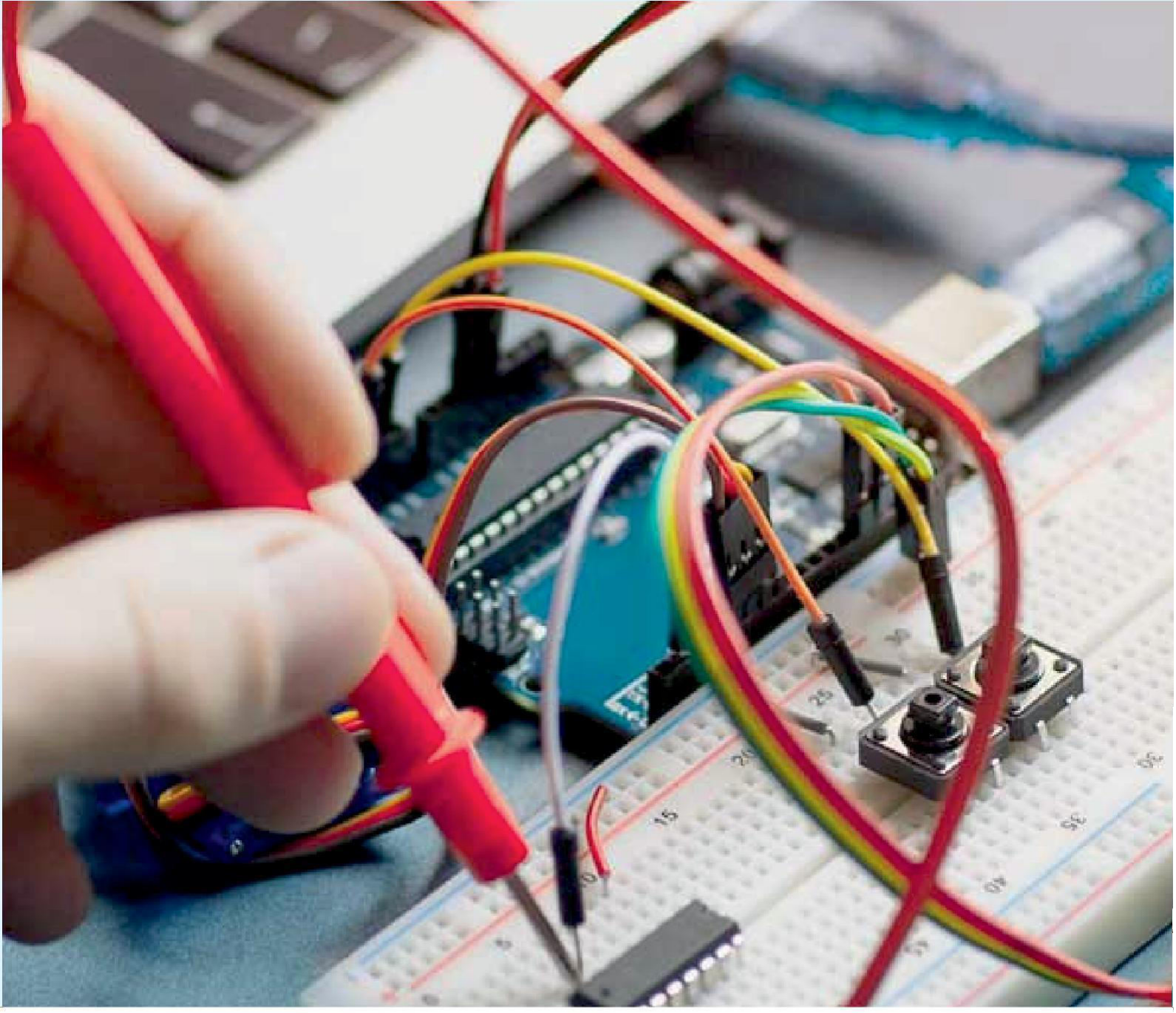

INNO SPACE
SJIF Scientific Journal Impact Factor

doi cross ref

ISSN INTERNATIONAL STANDARD SERIAL NUMBER INDIA

निस्केयर NISCAIR

International Journal of Advanced Research

in Electrical, Electronics and Instrumentation Engineering

9940 572 462 6381 907 438 ijareeie@gmail.com

Scan to save the contact details